

**Multiplicity Dependence of the Transverse
Momentum Spectrum for Centrally Produced Hadrons**

in Antiproton-Proton Collisions at $\sqrt{s} = 1.8$ TeV

T. Alexopoulos^(f), C. Allen^(e), E.W. Anderson^(c), H. Areti^(b),
S. Banerjee^(d), P.D. Beery^(d), N.N. Biswas^(d), A. Bujak^(e),
D.D. Carmony^(e), T. Carter^(a), P. Cole^(e), Y. Choi^(e),
R. De Bonte^(e), A. Erwin^(f), C. Findeisen^(f), A.T. Goshaw^(a),
L.J. Gutay^(e), A.S. Hirsch^(e), C. Hojvat^(b), V.P. Kenney^(d),
D. Koltick^(e), C.S. Lindsey^(c), J.M. LoSecco^(d), T. McMahon^(e),
A.P. McManus^(d), N. Morgan^(e), K. Nelson^(f), S.H. Oh^(a),
J. Piskarz^(d), N.T. Porile^(e), D. Reeves^(b),
R.P. Scharenberg^(e), B.C. Stringfellow^(e), S.R. Stampke^(d),
M. Thompson^(f), F. Turkot^(b), W.D. Walker^(a), C.H. Wang^(c),
D.K. Wesson^(a)

- (a) Department of Physics, Duke University, Durham, NC 27706
- (b) Fermi National Accelerator Laboratory,
P.O. Box 500, Batavia, IL 60510
- (c) Department of Physics, Iowa State University, Ames, IA 50011
- (d) Department of Physics, University of Notre Dame,
Notre Dame, In 46556
- (e) Department of Physics and Chemistry, Purdue University,
West Lafayette, IN 47907
- (f) Department of Physics, University of Wisconsin,
Madison, WI 53706

Submitted to Physical Review Letters.

ABSTRACT

The transverse momentum of charged particles produced within the pseudorapidity range $\eta = -0.36$ to $+1.0$ has been measured in $\bar{p}p$ collisions at $\sqrt{s} = 1.8$ TeV. The charged particle multiplicity of each event was measured with a 240 element cylindrical hodoscope system covering the range $-3.25 < \eta < 3.25$. The average transverse momentum as a function of the average charged particle density per unit of pseudorapidity is presented. Events are observed with average charged particle density as high as 32 per unit of pseudorapidity.

In this letter, we report the first results of experiment E735, performed at the CO intersection region of the Fermilab $\bar{p}p$ collider at a center of mass energy $\sqrt{s} = 1.8$ TeV. The experiment was designed to search for evidence of a phase transition of hadronic matter to a deconfined quark-gluon state. During the first running period from January to May 1987, 5 million triggers were collected from a total integrated luminosity of $\sim 1/3 \text{ nb}^{-1}$.

We report measurements of the correlation between the average transverse momentum, $\langle p_t \rangle$, and the charged particle multiplicity in the central rapidity region. The $\langle p_t \rangle$ may be interpreted as a measure of the temperature of the hadronic matter formed in the collisions, while the particle density in rapidity is proportional to its entropy density¹. Structure in the distribution of $\langle p_t \rangle$ versus multiplicity, in particular a rise in $\langle p_t \rangle$ followed by a plateau and a second rise after the plateau could be interpreted as one of the signatures of a phase transition in hadronic matter². Similar measurements at lower center of mass energies have previously been made in a cosmic ray experiment³, at the ISR⁴, and the S $\bar{p}p$ S collider⁵. There are also high energy, heavy ion programs now underway at CERN⁶ and Brookhaven using fixed targets.

Our detector⁷ consists of a 240 element multiplicity hodoscope surrounding the interaction region, a trigger system and a magnetic spectrometer at 90° which samples the charged particle spectrum with a solid angle of 0.5 sr.

The multiplicity hodoscope consists of a central barrel system and an upstream and downstream end cap. The barrel system has two halves, each with 48 counters parallel to the beam and covering the pseudorapidity range $-1.64 < \eta < 1.64$. The two end-cap hodoscopes consist of three rings each with 24 counters per ring and extend the pseudorapidity interval coverage to $-3.25 < \eta < 3.25$. The number of elements hit, N_h , in the barrel and endcap hodoscope systems is used to determine the charged particle multiplicity.

The trigger hodoscopes, with nine elements each, are located outside the multiplicity hodoscope covering the pseudorapidity interval $3 < |\eta| < 4.5$. All events were required to pass the minimum bias trigger defined as having at least one hit in both the upstream and downstream trigger hodoscopes, with each having an interaction time consistent with the $\bar{p}p$ crossing time. High multiplicity events were enhanced with an online trigger processor. The acceptance of events due to trigger bias was studied as a function of multiplicity and corrected with a Monte Carlo simulation of the experiment.

The spectrometer arm consists of drift chambers and a dipole magnet with a 50 MeV/c transverse momentum kick. The spectrometer covers the pseudorapidity range $-0.36 < \eta < 1.0$ with an azimuthal angular acceptance of 18 degrees. Particle trajectories are measured using eight drift chamber planes within the magnet aperture followed by fourteen drift chamber planes behind the magnet.

To understand the effect of beam-gas collisions and other background processes on the trigger, use was made of machine fills with antiproton bunches missing. Events obtained when a proton bunch crossed the interaction region without the corresponding antiproton bunch were used to study the characteristics of beam-gas events. An algorithm was devised to remove these events and isolate true $\bar{p}p$ collisions using the multiplicity hodoscope. It was based on the forward-backward asymmetry of the hit distribution and the difference in the timing structure between $\bar{p}p$ and background events. After applying the algorithm, about 2% of the remaining events are from non $\bar{p}p$ interactions. We find no appreciable variation of this background with event multiplicity.

Tracks are reconstructed behind the magnet, then traced through the magnet and matched with hits in the magnet chambers. After reconstruction, a track was rejected if the momentum was less than 150 MeV/c, or if the χ^2 per degree of freedom was greater than three or if the fitted momentum error was greater than $2 \Delta p$ (Eq. 1 below).

A Monte Carlo simulation was used to study the momentum resolution, the momentum dependence of the magnetic acceptance and pattern recognition efficiency. The detector hits were simulated including the effect of the position resolution of the drift chambers, multiple scattering and decays in flight. All particles were assumed to be pions. The overall acceptance, product of the magnetic acceptance and the reconstruction

efficiency, varies from 83% at $p = 150$ MeV/c to 95% at $p = 300$ MeV/c. The acceptance is normalized to be 100% at $p = 1$ GeV/c. For the momentum resolution, we parameterize the RMS momentum error by the form

$$\Delta p/p = (ap^2 + b\beta^{-2})^{1/2} \quad (1)$$

where $\beta = v/c$ and p is in GeV/c. From the Monte Carlo, we found a and b are approximately 0.0018.

After reconstruction, tracks not coming from the interaction point were eliminated using vertex cuts. The observed interaction vertex has a Gaussian distribution along the beam direction with a standard deviation of 30 cm. Two tracks were considered to have originated from a single interaction vertex (i.e. "intersected") if they lay within 2 cm of each other at the beam line. Events with two or more intersecting spectrometer tracks were accepted only if their average vertex at the beam line was within 10 cm of the interaction vertex as determined by the trigger hodoscopes. The RMS error in the determination of the vertex position using the trigger hodoscopes is 5 cm. For events in which either a single spectrometer track was observed or no intersection was found at the beam line between multiple tracks, only those tracks which crossed the beam line axis within 10 cm of the trigger hodoscope vertex were accepted.

We define N_g as the number of tracks passing the above selection criteria. We estimate that about 10% of the tracks in the all-track sample ($N_g \geq 1$) and less than 5% in the

intersecting-track sample ($N_g \geq 2$) are background. The ratio of accepted positive particles to accepted negative particles for $\bar{p}p$ interactions is expected to be 1.04 from the Monte Carlo study which was used to calculate the spectrometer arm acceptance. In the all-track sample we observe a ratio of 1.10, hence it appears that the background tracks are predominately positive. The ratio for the intersecting-track sample is 1.04 consistent with the Monte Carlo result.

Since N_h is affected by background tracks as well as by the effects of saturation due to the finite number of elements in the hodoscope systems, it must be corrected to obtain the true charged particle multiplicity N_c . A Monte Carlo model was used to obtain N_c over the interval $|\eta| < 3.25$. The model produced particles uniformly both in azimuth and pseudorapidity over the acceptance of the multiplicity hodoscope. The effect of background particles was included by adding hodoscope hits equal to the ratio of background tracks to true tracks as observed in the spectrometer arm before vertex cuts. This ratio was found to vary linearly with N_h from 0.2 for $N_h = 30$ to 0.3 for $N_h = 150$. The value of N_c so determined has an estimated uncertainty of $\sim 10\%$.

As a check of the Monte Carlo program, the average number of observed tracks $\langle N_g \rangle$ in the spectrometer as a function of N_h was also calculated, and is shown in Figure 1 for $N_g \geq 1$, as well as for $N_g \geq 2$. The solid curves are obtained from the Monte Carlo calculation. The agreement between the calculation

and the data allows us to present our results as a function of N_c and $\langle dN_c/d\eta \rangle$ which is calculated by dividing N_c by 6.5 units of pseudorapidity. N_c as a function of N_h is plotted in Figure 2.

In Figure 3, the acceptance corrected single particle distribution $1/p_t \, dN/dp_t$ is plotted as a function of p_t for two different multiplicity intervals, for N_c less than 45 and N_c greater than 110. The p_t spectrum is observed to flatten in the higher multiplicity interval.

In Figures 4 and 5, $\langle p_t \rangle$ is plotted both as a function of N_c and $\langle dN_c/d\eta \rangle$ averaged over the acceptance of the multiplicity hodoscope. In Figure 4, positive and negative tracks are plotted separately for $N_h \geq 1$. The difference in shape between the positive and negative particles is probably due to the excess of background tracks in the positive sample. Also plotted are the negative tracks after correcting for the unobserved particles with $p_t < 150$ MeV/c as discussed below. For comparison, the results from UA1 measurement⁵ at $\sqrt{s} = 540$ GeV are also plotted. The shape of our data is consistent with UA1 data in the multiplicity region where they overlap.

The contribution from particles with p_t less than 150 MeV/c was calculated by extrapolating the dN/dp_t^2 distribution to $p_t = 0$ using the form $\exp(-bp_t)$. The value of b is obtained by fitting the distribution from $p_t = 0.15$ GeV/c to 0.50 GeV/c. The correction factor was obtained for different multiplicity

intervals and found to be almost constant over the entire multiplicity region. Using this technique, an overall $\langle p_t \rangle$ of 0.46 ± 0.01 GeV/c was obtained for particles with p_t less than 3.0 GeV/c from the sample of minimum bias events. Assuming the exponential p_t extrapolation is correct, the error is dominated by an estimated effect of background tracks in the sample.

In Figure 5 only those events with $N_{\pm} \geq 2$ are plotted averaged over the momentum range $0.15 \text{ GeV/c} < p_t < 3.0 \text{ GeV/c}$. This subset of events has fewer background tracks as was discussed earlier. Because the $\langle p_t \rangle$ distribution of positive and negative particles are very similar, only their sum is plotted in the figure.

As shown in the figures, $\langle p_t \rangle$ rises steeply followed by a plateau like region. Then there is an apparent step⁸ at $\langle dN_c/d\eta \rangle = 15$ followed by a gradual rise.

In summary, we have measured $\langle p_t \rangle$ at $\sqrt{s} = 1.8 \text{ TeV}$ up to $\langle dN_c/d\eta \rangle$ as large as 32. This is about twice that measured in previous collider experiments. Applying Bjorken's formula⁹ this corresponds to an energy density $\epsilon = 3.8 \text{ GeV/fm}^3$. The new data raise the possibility of interesting structure in the higher range of $\langle dN_c/d\eta \rangle$.

We would like to thank the administrative and technical staff at Fermilab and our respective universities for their support of the experiment. Participation of M. Duong-Van in the proposal is greatly appreciated. This work was supported in part by the United States Department of Energy and the National Science Foundation.

REFERENCES

- 1) L.D. Landau, Izv. Akad. Nauk. SSSR, Ser. Fiz. 17 (1953) 51.
- 2) L. Van Hove, Phys. Lett. 118B, 138 (1982).
- 3) T.H. Burnett et al., Phys. Rev. Lett., 57, 3249 (1986).
- 4) A. Breakstone et al., Z. Phys. C. 33, 333 (1987)
- 5) UA1 Collaboration, Phys. Lett. 118B, 167 (1982).
- 6) P. Giubellino, Proceedings of the Vanderbilt Conference 1987
(to be published).
- 7) FNAL E735 Collaboration, Proceeding of Multiparticle
Dynamics 1986, (p. 839) World Scientific Publication,
Edited by N. Markytan, W. Majoretto, J. MacNaughton.
- 8) If we fit 4 points on either side of the step in Figure 5
with a horizontal line, then the step is 36 ± 5 MeV/c. A
straight line fit through the 8 points yields a
 $\chi^2/\text{D.O.F.} = 3.0$.
- 9) J.D. Bjorken, Phys. Rev. D27, (1983) 140.

FIGURE CAPTIONS

Figure 1: Number of accepted tracks per event in the spectrometer arm as function of hodoscope multiplicity compared with Monte Carlo predictions: for all tracks ($N_h \geq 1$) and for all intersecting tracks ($N_h \geq 2$). The solid curve is the Monte Carlo calculation.

Figure 2: N_c as a function of N_h for $|\eta| < 3.25$ derived from a Monte Carlo calculation. The error bars shown only at a few points are the RMS spread of the $N_c(N_h)$ values for a given $N_h(N_c)$.

Figure 3: The normalized single particle $1/p_t \, dN/dp_t$ distribution for two different N_c regions.

Figure 4: $\langle p_t \rangle$ as a function of N_c and $\langle dN_c/d\eta \rangle$ for all positive tracks and all negative tracks averaged over the interval $0.15 \text{ GeV}/c < p_t < 3.0 \text{ GeV}/c$. The corrected $\langle p_t \rangle$ of negative particles includes unobserved particles with $p_t < 0.15 \text{ GeV}/c$ (see text). Last few uncorrected data points are omitted for clarity. The UA1 data⁵ is from $\sqrt{s} = 540 \text{ GeV}/c$.

Figure 5: $\langle p_t \rangle$ as a function of N_c and $\langle dN_c/d\eta \rangle$ for all charged particles with $N_h \geq 2$, averaged over the interval $0.15 \text{ GeV}/c < p_t < 3.0 \text{ GeV}/c$.

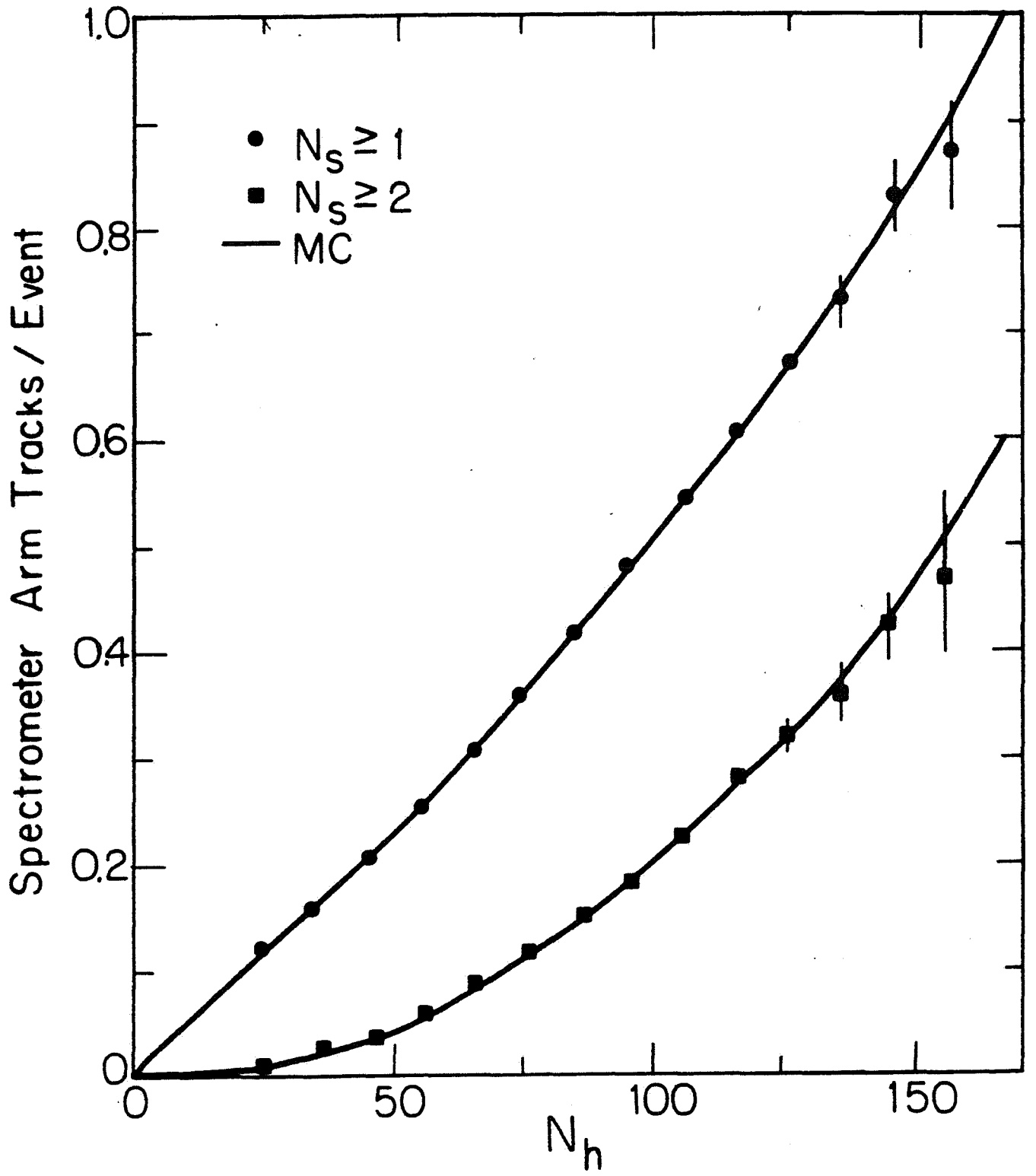


Figure 1

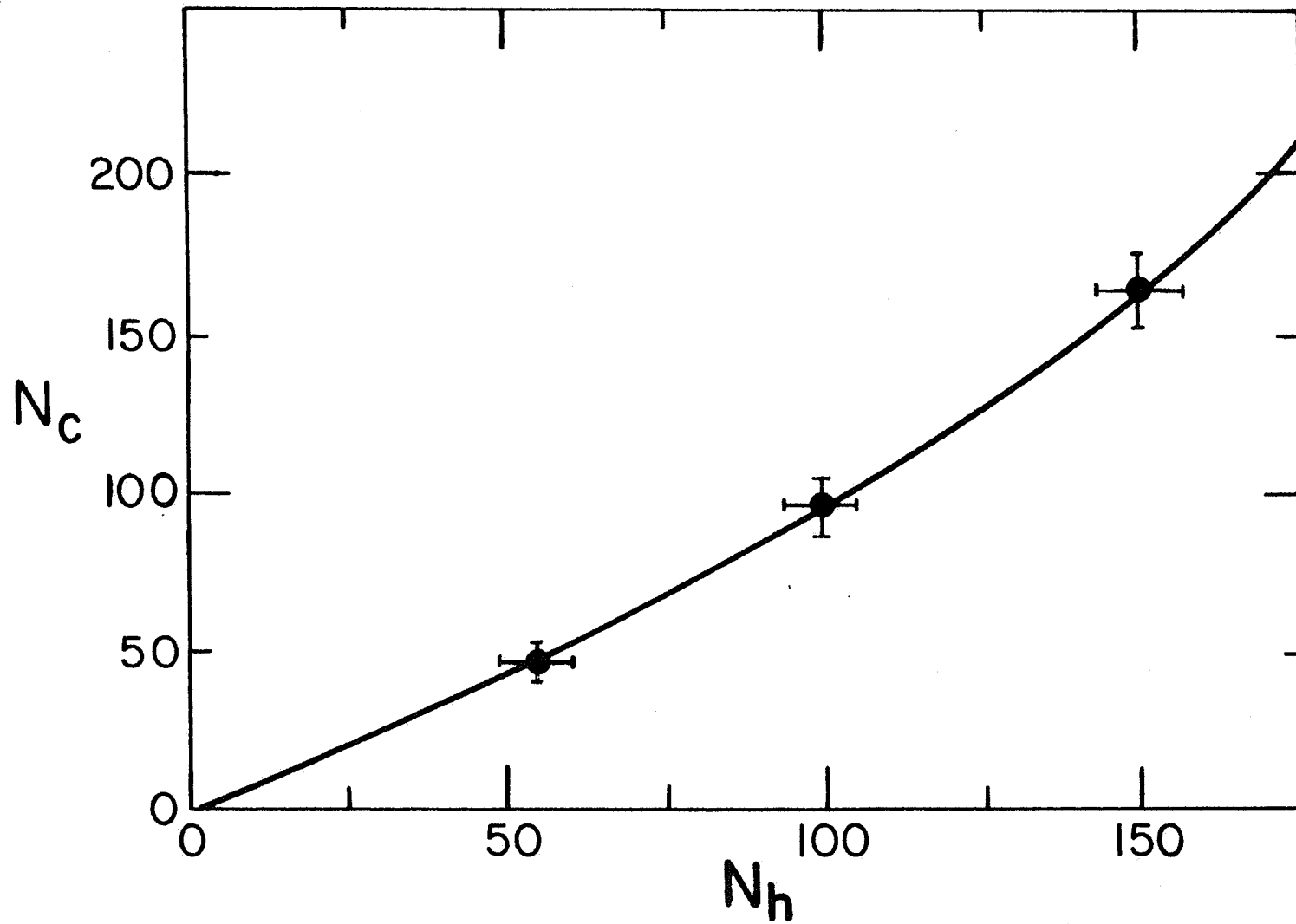


Figure 2

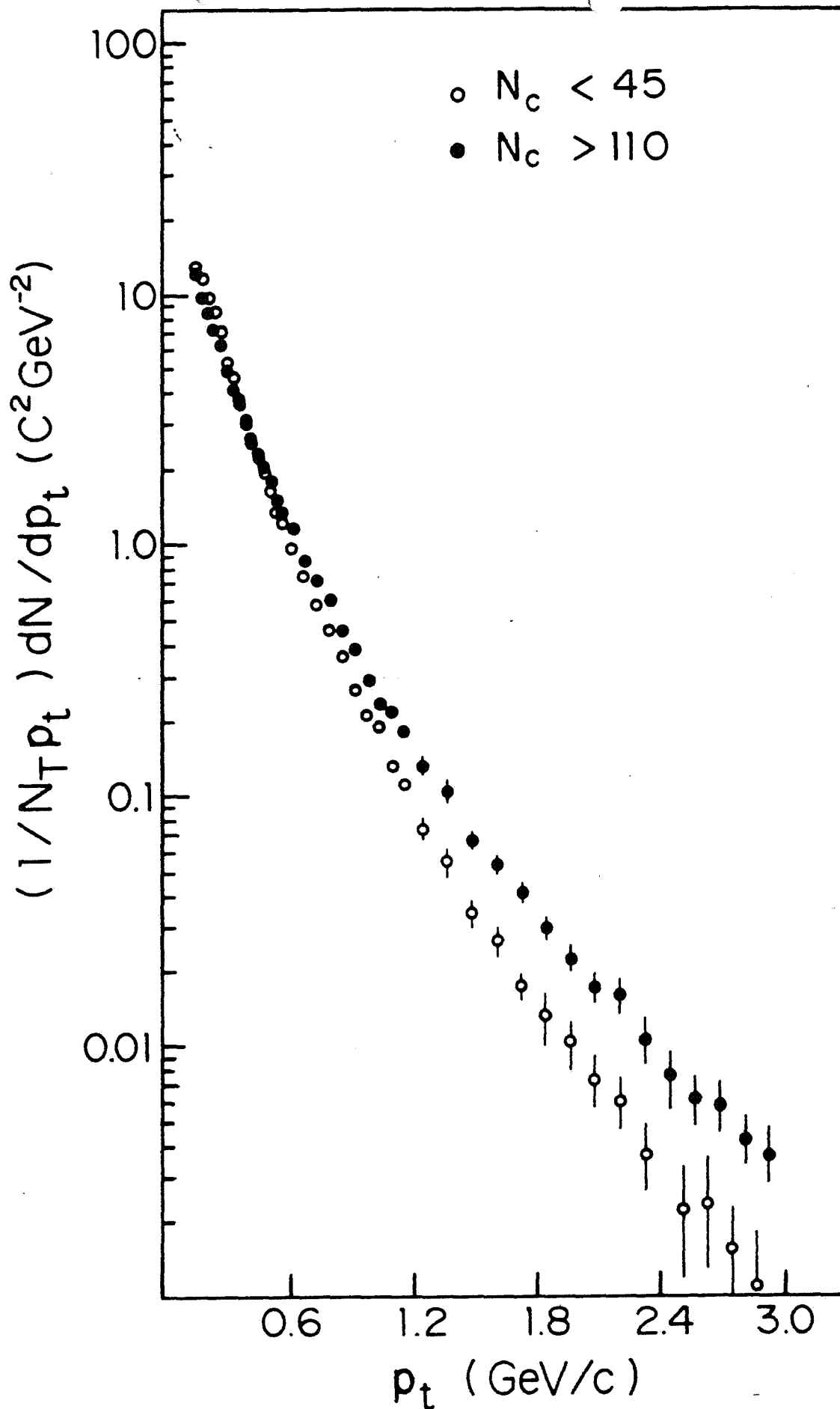


Figure 3

$$\langle dN_C/d\eta \rangle$$

5 10 15 20 25 30

$N_s \geq 1$

- * positive
- ▲ negative } uncorrected
- negative — corrected
- — UA1

$$\langle p_t \rangle \text{ (GeV/c)}$$

0.7
0.6
0.5
0.4
0.3

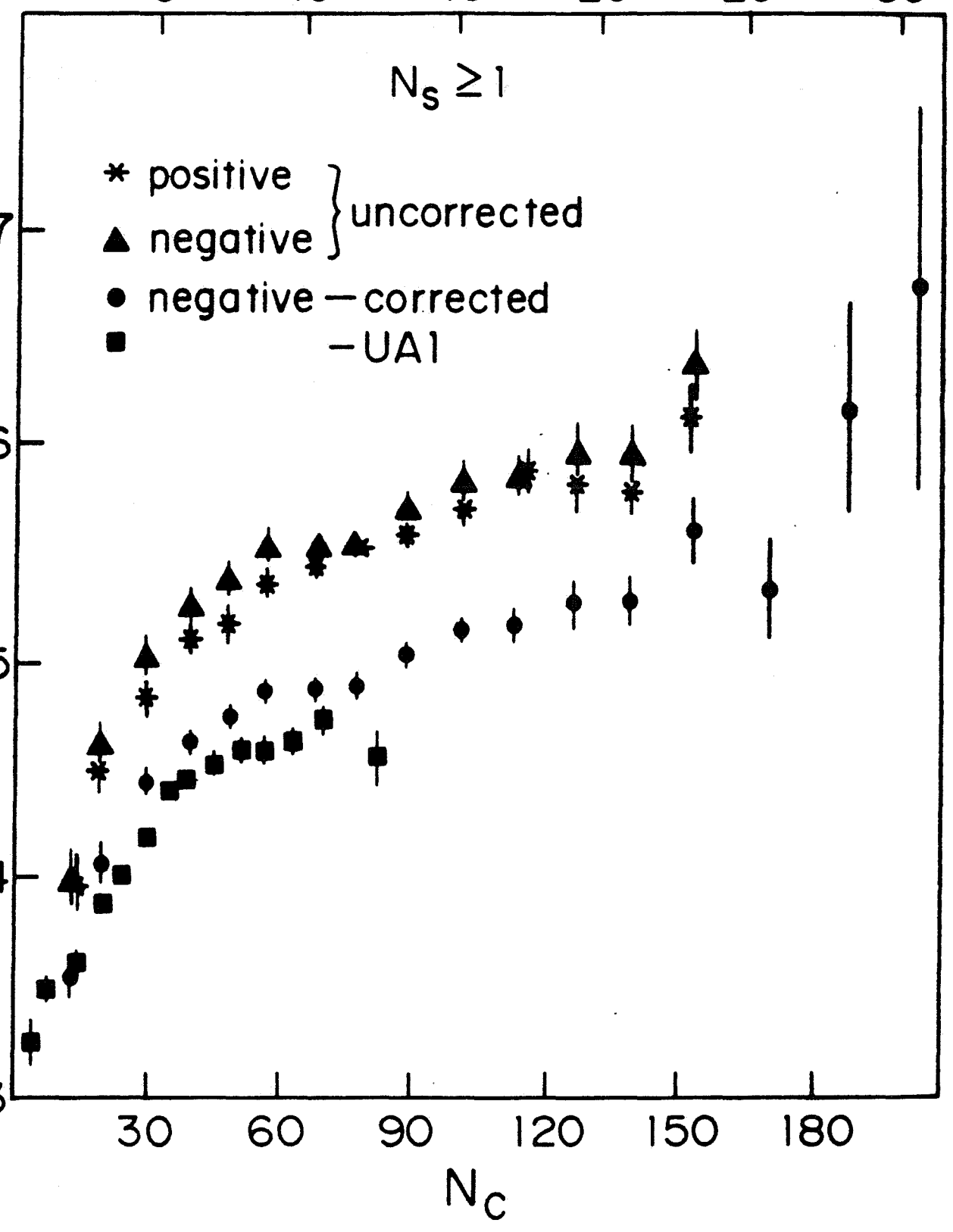


Figure 4

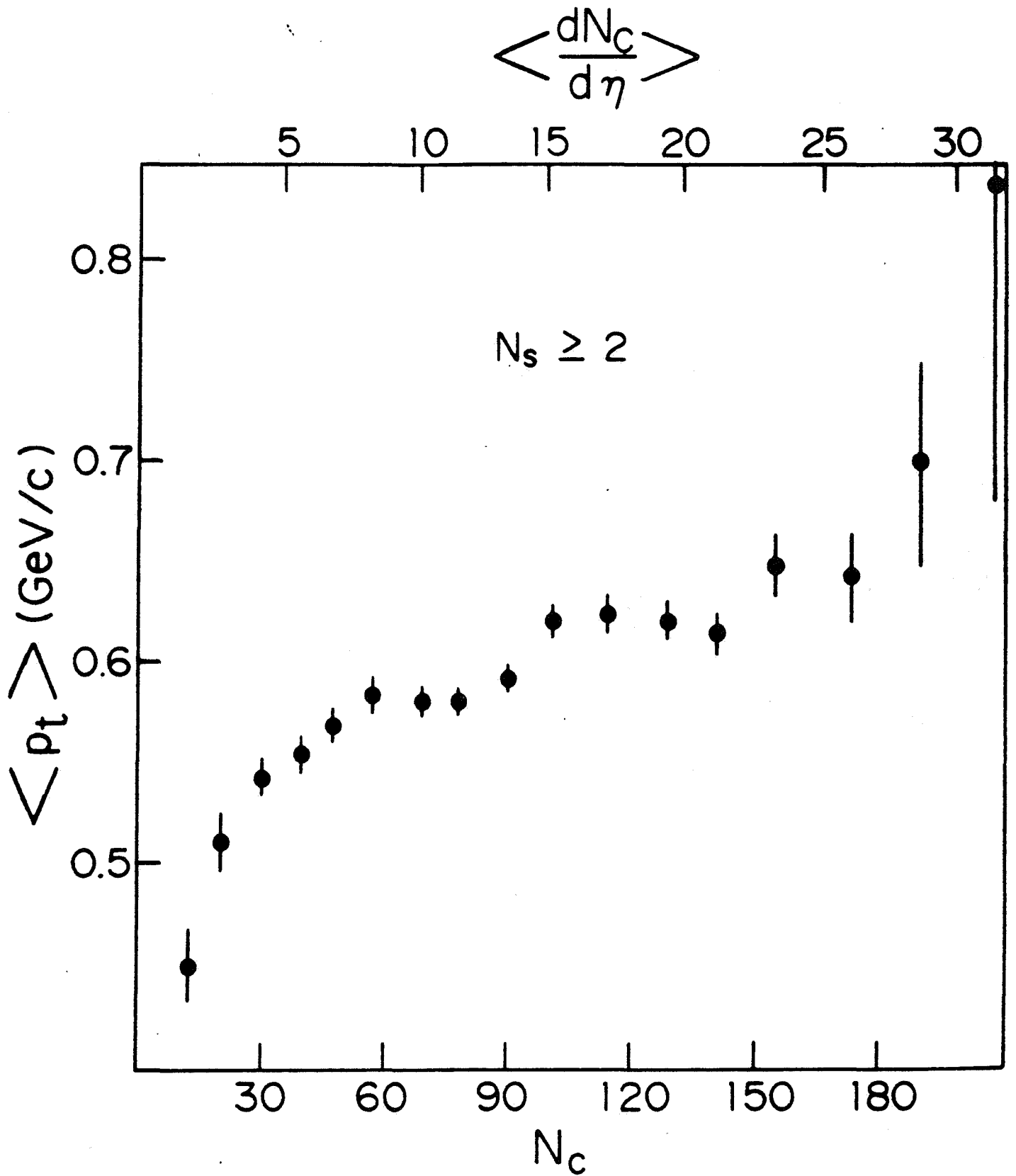


Figure 5